Published online 20 March 2012 *Nucleic Acids Research, 2012, Vol. 40, No. 13* ***6187–6198***
doi:10.1093/nar/gks254

Collaborative coupling between polymerase and helicase for leading-strand synthesis

Maria Manosas[1,2,3], Michelle M. Spiering[4], Fangyuan Ding[1,5], Vincent Croquette[1,5,*] and Stephen J. Benkovic[4,*]

[1]Département de Physique, Laboratoire de Physique Statistique, Ecole Normale Supérieure, Université Pierre et Marie Curie Université Paris 06, Université Paris Diderot, Centre National de la Recherche Scientifique, Paris 75005, France, [2]Departament de Física Fonamental, Universitat de Barcelona, Barcelona 08028, [3]CIBER-BBN de Bioingenieria, Biomateriales y Nanomedicina, Instituto de Sanidad Carlos III, Madrid 28029, Spain, [4]Department of Chemistry, The Pennsylvania State University, University Park, PA 16802, USA and [5]Département de Biologie, Ecole Normale Supérieure, Paris 75005, France

Received January 15, 2012; Revised March 5, 2012; Accepted March 6, 2012

ABSTRACT

Rapid and processive leading-strand DNA synthesis in the bacteriophage T4 system requires functional coupling between the helicase and the holoenzyme, consisting of the polymerase and trimeric clamp loaded by the clamp loader. We investigated the mechanism of this coupling on a DNA hairpin substrate manipulated by a magnetic trap. In stark contrast to the isolated enzymes, the coupled system synthesized DNA at the maximum rate without exhibiting fork regression or pauses. DNA synthesis and unwinding activities were coupled at low forces, but became uncoupled displaying separate activities at high forces or low dNTP concentration. We propose a collaborative model in which the helicase releases the fork regression pressure on the holoenzyme allowing it to adopt a processive polymerization conformation and the holoenzyme destabilizes the first few base pairs of the fork thereby increasing the efficiency of helicase unwinding. The model implies that both enzymes are localized at the fork, but does not require a specific interaction between them. The model quantitatively reproduces homologous and heterologous coupling results under various experimental conditions.

INTRODUCTION

DNA replication, a fundamental process of all living organisms, is carried out by a multiprotein complex known as the replisome (1). In the replisome, the polymerase collaborates with the helicase to drive both leading- and lagging-strand DNA synthesis. DNA polymerases can only synthesize nascent DNA in the 5′–3′ direction; therefore, the leading-strand holoenzyme copies the DNA template continuously, whereas the lagging-strand holoenzyme copies the DNA template in short, ~1 Kbp segments know as Okazaki fragments. Lagging-strand DNA synthesis requires the activity of a primase that synthesizes RNA primers for initiating repetitive Okazaki fragment synthesis and the presence of single-stranded DNA-binding protein that protects the ssDNA from degradation. In contrast, leading-strand DNA synthesis only requires the coordinated action of the helicase and the holoenzyme.

In vitro, replicative helicases, like the gp41 helicase from bacteriophage T4, are capable of unwinding a DNA replication fork when operating independently, but with a reduced processivity and at a rate far slower than the replication rate of an entire replisome (2). Likewise, independent replicative polymerases, like the T4 holoenzyme consisting of the gp43 polymerase and gp45 trimeric clamp loaded by the gp44/62 clamp-loader complex, are capable of extending a primer/template substrate, but are generally very inefficient at strand displacement synthesis (3). However, functional coupling between these two enzymes leads to rapid and processive duplex unwinding and leading-strand synthesis akin to the activity of the replisome (4).

Understanding of the exact mechanism of this coupling phenomenon remains limited, despite several previous studies. Delagoutte and von Hippel (5) investigated the polymerase–helicase coupling in the T4 system concluding a processive 'trailing' DNA polymerase was sufficient to improve the processivity and unwinding activity of the gp41 helicase. The authors found no physical interaction between the gp43 polymerase and gp41 helicase determining instead that the functional coupling depended on interactions modulated by the DNA replication fork which mutually stabilized each protein at their respective

*To whom correspondence should be addressed. Tel: +1 814 865 2882; Fax: +1 814 865 2973; Email: sjb1@psu.edu
Correspondence may also be addressed to Vincent Croquette. Tel: +33 01 44 32 34 92; Fax: +33 01 44 32 34 33; Email: vincent.croquette@lps.ens.fr

sites of action. Specifically, the 'trailing' DNA polymerase trapped the ssDNA product of the helicase unwinding activity, preventing the separated strands from reannealing and diminishing the occurrence of helicase 'slippage', thereby increasing the unwinding rate.

Stano *et al.* (6) investigated the holoenzyme–helicase coupling in the T7 system concluding that DNA synthesis provided the driving force to accelerate DNA unwinding by a helicase. The authors report that the strand displacement DNA synthesis by the T7 holoenzyme depended on the unwinding activity of the helicase to supply ssDNA template; however, it was the rapid trapping of the ssDNA bases by the DNA synthesis activity of the holoenzyme which drove the helicase to move forward through duplex DNA at speeds similar to those observed along ssDNA. Nevertheless, the detailed mechanisms by which the holoenzyme generates a driving force for the helicase and, in turn, the helicase activates the holoenzyme DNA synthesis activity remain unknown.

In this work, we investigate the activity of several holoenzymes and the T4 helicase individually and in collaboration during DNA synthesis on DNA hairpins using magnetic tweezers to manipulate single DNA molecules. We found that the T4 homologous coupled system was very efficient and DNA synthesis advanced at the maximum rate without exhibiting fork regression or pauses, which was in stark contrast to the isolated enzymes. DNA synthesis and unwinding activities were coupled at low forces, but became uncoupled displaying separate helicase and holoenzyme activity at high forces or low dNTP concentration. To explain these results, we propose a collaborative model in which the helicase releases the fork regression pressure on the holoenzyme allowing it to adopt a processive polymerization conformation and the holoenzyme destabilizes the first few base pairs of the fork thereby increasing the unwinding efficiency of the helicase. The collaborative model implies that both enzymes are localized at the fork, but does not feature a protein–protein interaction. The proposed model quantitatively reproduces the efficient T4 homologous coupling as well as the heterologous coupling between the T7 holoenzyme and the T4 helicase.

MATERIALS AND METHODS

Proteins and DNA hairpin substrate

The T4 proteins, wild-type (wt) and exonuclease-deficient gp43 polymerase (7), gp45 clamp (8), gp44/62 clamp-loader complex (9), gp41 helicase (10) and wild-type gp32 single-stranded DNA-binding protein and truncation mutants gp32-A and gp32-B (11) were purified as previously described. The Φ29 DNA polymerase and the T7 DNA polymerase (T7 gp5 in a 1:1 complex with thioredoxin) were purchased from New England Biolabs. The 1.2 Kbp DNA hairpin substrate was constructed as previously described (12).

Single-molecule assay

We used a PicoTwist magnetic tweezers instrument (www.picotwist.com) to manipulate individual DNA hairpin molecules tethered between a glass surface at the 3′ end and a magnetic bead at the 5′ end. The glass surface was treated with anti-digoxigenin antibody (Roche) and passivated with bovine serum albumin. Streptavidin-coated Dynal magnetic beads (Invitrogen) were 1 μm in diameter. T4 holoenzyme (10 nM polymerase, clamp loader, and clamp trimer), T4 hexameric helicase (10 nM), T4 ssDNA-binding protein gp32, gp32-A or gp32-B (200 nM), T7 polymerase (500 units/mL) or Φ29 polymerase (500 units/mL) were flowed into the chamber diluted in the reaction buffer [25 mM Tris–OAc pH 7.5, 150 mM KOAc, 10 mM $Mg(OAc)_2$, 1 mM dithiothreitol, 100 μM dNTPs and 2.5 mM ATP].

The DNA hairpins are manipulated by capturing the bead in a magnetic trap generated by a pair of permanent magnets. The applied force is controlled by varying the distance of the magnets from the sample. Videomicroscopy is used to track the position of the magnetic bead in three dimensions with nanometer resolution at 30 Hz at 37°C, from which the extension of the DNA molecule and the strength of the stretching force is deduced (13). A calibration curve of the applied force versus the vertical position of the magnets was used to exert forces with 10% error on the DNA molecules.

Single-molecule data analysis

Raw data, corresponding to the real-time evolution of the DNA extension in nm, was converted into the number of base pairs unwound by helicase or the number of base pairs synthesized or excised by holoenzyme or polymerase using a calibration factor determined from the elastic properties of ssDNA and dsDNA [Figures 1 and 2; Supplementary Figure S2 in (14)]. Instantaneous enzymatic rates were obtained from a linear fit to the traces filtered with a third-order Savitzky–Golay filter over a sliding time window of varying size depending on the applied force. For helicase activity, slippage events, involving the regression of the fork by ≥ 10 bp, were directly detected from the extension traces. Instantaneous unwinding and translocation rates were calculated from sections of the experimental traces where slippage events were disregarded. For holoenzyme and polymerase activity, separate velocity distributions for primer extension activity and strand displacement activity were determined from the histogram of the instantaneous rate measured during the respective region of each data trace. The velocity distributions were fit to the sum of the appropriate number of Gaussians (14). For the strand displacement data, the relative occupancy of the three observed phases, synthesis, pausing and degradation was determined from the ratio of the areas under each peak of the velocity distribution.

Model

Betterton and Jülicher (15,16) proposed a framework to describe DNA unwinding by helicases. In this model, the dynamics of the DNA fork/helicase system are governed by the DNA base pair opening and closing rates, α and β, and the helicase intrinsic forward and backward

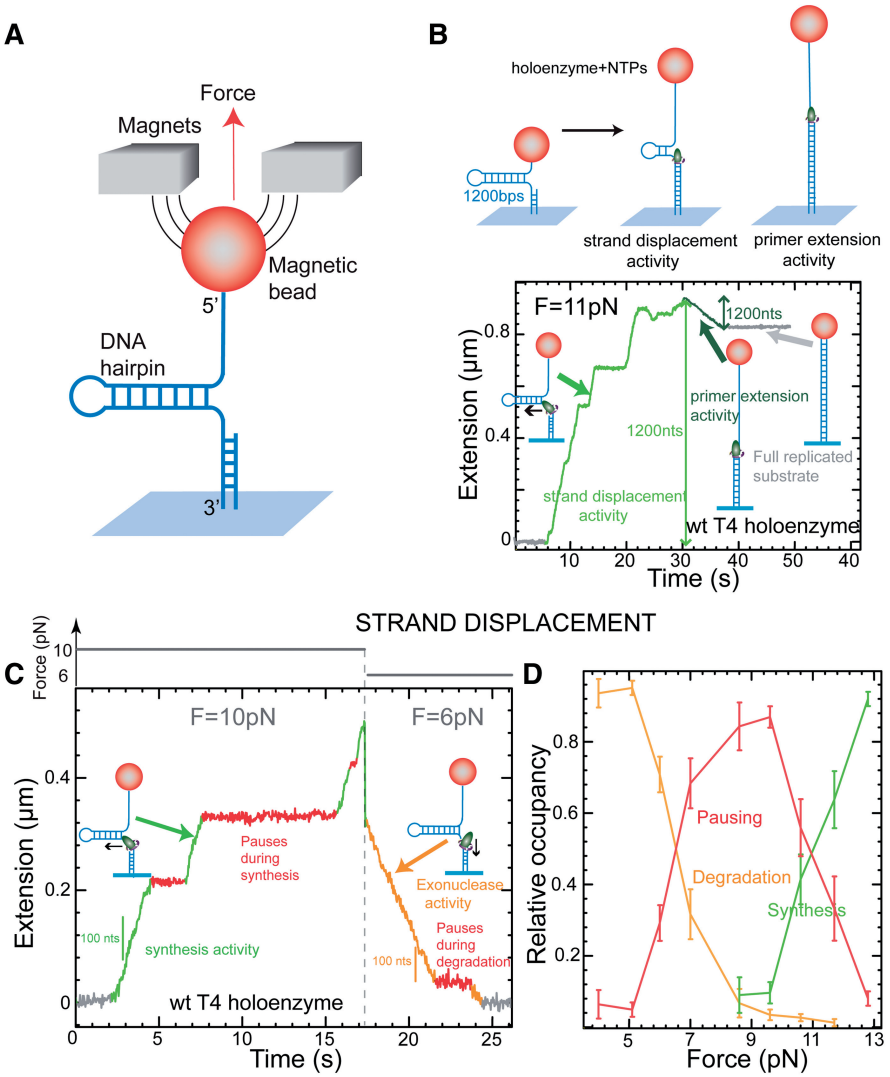

Figure 1. T4 holoenzyme activity on a DNA hairpin substrate. (**A**) Schematic representation of the experimental set-up. A 1.2 Kbp DNA hairpin substrate was tethered between the glass surface and a magnetic bead held in a magnetic tweezers. (**B**) Schematics (upper panel) and experimental trace (lower panel) corresponding to the wt T4 holoenzyme loaded at the 3′ end of the primer displaying strand displacement (partially opened hairpin) and primer extension activities (opened hairpin). The change in extension observed during the two phases corresponding to the polymerization of about ~1200 nt was used to compute the conversion factor between the measured extension change and the number of incorporated nucleotides by the holoenzyme at a given force. Whereas the strand displacement phase (light green) resulted in an increase in the molecule's length (each base synthesized results in the opening of 2 nt), the primer extension phase (dark green) resulted in a continuous decrease of the molecule's length (dsDNA is shorter than ssDNA above 6 pN of force) until the substrate was fully replicated and the molecule's extension remained constant. (**C**) Experimental trace of wt T4 holoenzyme strand displacement activity demonstrating the force-induced switch from DNA synthesis at high force (light green) to DNA degradation at low force (yellow). Pauses were observed during both types of activities (shown in red). Bars show the extension change corresponding to the synthesis or degradation of 100 nt. (**D**) Relative occupancy of the three phases, synthesis, pausing and degradation, shown as a function of the applied force.

translocation rates along ssDNA, k^+ and k^-. The link between the helicase movement and the DNA base pair opening comes from the fact that these rates depend on the relative position between the helicase and the DNA fork, e.g. the fork cannot reanneal if the helicase is adjacent to it. The model depends strongly on parameters such as the step size of the enzyme (n), the ability of the enzyme to move backwards ($k^- \neq 0$) and the enzyme's DNA-destabilization potential (ΔG_a, m). In addition to describing helicase movement, we have used the same model to describe the holoenzyme during strand displacement activity with the exception that the backward movement was prohibited ($k^- = 0$). Details of the model are presented in Supplementary Materials.

For the coupled holoenzyme-helicase reaction, we utilized a combined model where the relative position of the enzymes was not imposed, thereby evaluating configurations with the helicase ahead of the holoenzyme ($x_{hel} > x_{pol}$) and the helicase behind the holoenzyme ($x_{hel} < x_{pol}$). In our model, only the enzyme in the leading position was considered to experience the effect of the regression force generated by the DNA fork. If the helicase was ahead of the holoenzyme, then the helicase was allowed to move forward and backwards, but the

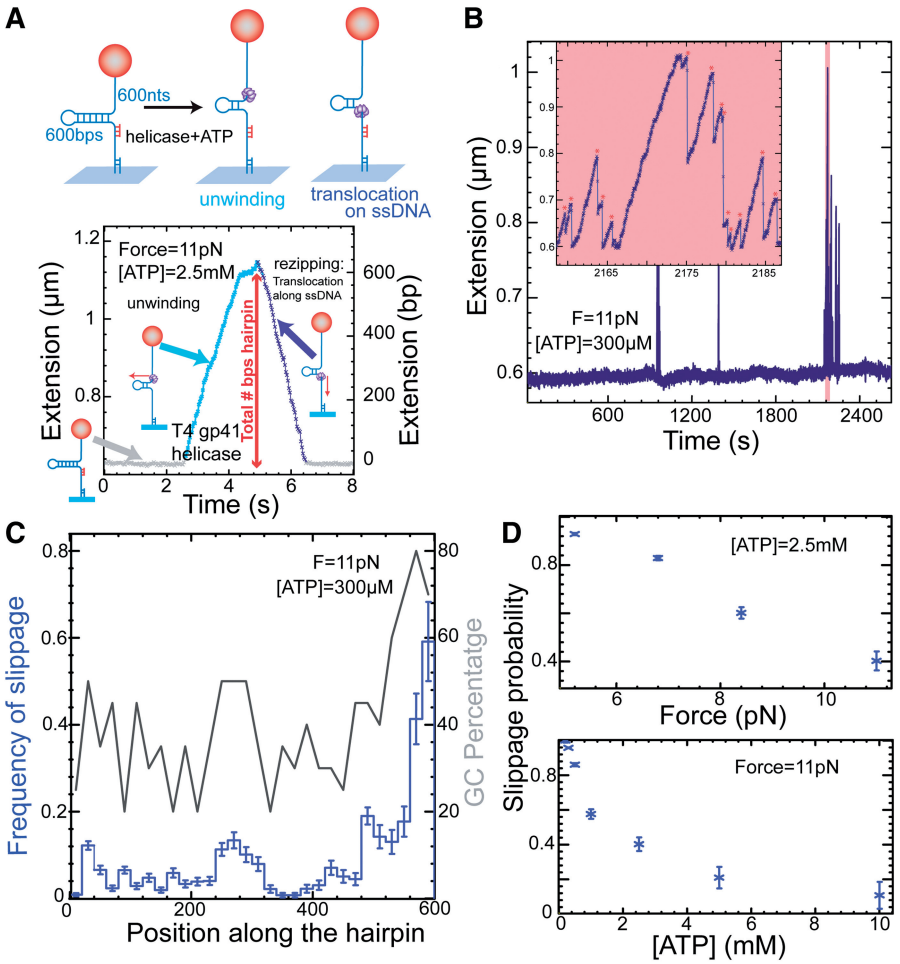

Figure 2. T4 helicase activity on a DNA hairpin substrate. (**A**) Schematics (upper panel) and experimental trace (lower panel) corresponding to the T4 helicase loaded on the 5′ ssDNA tail of the hairpin displaying DNA unwinding activity followed by ssDNA translocation activity concomitant with hairpin reannealing. The measured extension change (left axis) is converted to the number of base pairs unwound (right axis) by assigning the full length of the hairpin to the maximum number of unwinding events. (**B**) Bursts of helicase activity were observed every tens of minutes ensuring the monitoring of a single helicase complex (10–20 nM gp41 and 300 μM ATP). Inset: Enlargement of the experimental trace exhibiting repeated cycles of unwinding and slippage (red asterisk). (**C**) The frequency of helicase slippage events (blue) correlated with the percent GC content of the substrate (grey) when plotted against the corresponding position of the DNA substrate. The error bars are proportional to the inverse of the square root of the number of points for each individual bin. The number of molecules and enzymatic traces analysed is $N_{mol} = 9$ and $N = 288$, respectively. (**D**) The percentage of experimental traces which exhibited helicase slippage events as a function of the applied force (upper panel) and the ATP concentration (lower panel) are shown. Error bars are the SEM. The number of molecules and enzymatic traces analysed varies between $N_{mol} = 17$–42 and $N = 163$–489, respectively, depending on the force and ATP condition.

holoenzyme was considered to remain in the active *pol* state (i.e. $k_{pol}^{-} = 0$). If the holoenzyme was in the leading position, then transitions from the *pol* state to the *exo* state of the holoenzyme were allowed; in order to simplify the model, we assumed that, at low forces where coupling is observed (<6 pN), the switch from the *pol* state to the *exo* state occurred instantaneously (i.e. $k_{pol}^{+} = 0, k_{pol}^{-} \neq 0$). Details of the model are presented in Supplementary Materials.

RESULTS

Experimental set up

To investigate the enzyme activity of the coupled holoenzyme and helicase complex as well as their uncoupled activities for comparison, we used magnetic tweezers to apply mechanical tension to DNA hairpin substrates attached between magnetic beads and a glass surface (Figure 1A) and monitored the end-to-end distance change as the DNA hairpin was opened and replicated to dsDNA. Increasing the applied mechanical force served as a means to assist the molecular motors to open the DNA hairpin and thus replace a partner in the collaborative work. We performed experiments at forces <14 pN; conditions under which the hairpin was mechanically stable [Supplementary Figure S1 in (14)]. The hairpin construct has a DNA primer hybridized to the 3′ tail that can be extended by the holoenzyme while opening the DNA fork allowing us to investigate both the strand displacement and the primer extension activities of the

holoenzyme (Figure 1B). We have studied the activity of four holoenzymes including the wild-type T4 holoenzyme (gp43 polymerase and gp45 trimeric clamp) from polymerase family B; a mutant T4 holoenzyme (gp43exo polymerase and gp45 trimeric clamp), which lacks the exonuclease activity; the wild-type T7 holoenzyme (gp5 polymerase and *Escherichia coli* thioredoxin) from polymerase family A and the Φ29 polymerase also from polymerase family B. The hairpin construct also has a 5′ ssDNA tail where T4 hexameric helicase is able to load allowing us to investigate both the unwinding and ssDNA translocation activity of the helicase (Figure 2A) as previously reported (17). The number of incorporated nucleotides or unwound base pairs was obtained by dividing the observed change in DNA extension by the expected change in DNA extension resulting from the incorporation of a single nucleotide or the unwinding of a single base pair [Supplementary Figure S2A and (14)]. By including both the holoenzyme and helicase proteins in our assays, we were able to investigate their coupled activity mimicking rapid, processive leading-strand DNA synthesis.

T4 and T7 replicative holoenzymes favour exonuclease activity during strand displacement synthesis

DNA synthesis by a holoenzyme on a DNA hairpin presents two phases. Initially, the holoenzyme has to open a base pair to incorporate a new nucleotide (strand displacement synthesis activity). This phase gives rise to a large change in extension, typically ~0.8 nm for a nucleotide incorporated at 10 pN. After reaching the end of the loop region, the enzyme only needs to extend the primer (primer extension activity). This second phase results in a moderate change in extension as a consequence of the different elastic properties of ssDNA and dsDNA (typically ~−0.1 nm for a nucleotide incorporated at 10 pN). After the primer extension phase, the substrate has been fully replicated and the extension remains constant (Figure 1B). A detailed study of the strand displacement and primer extension activities of the T4 and T7 replicative holoenzymes is presented in the companion article (14). Primer extension synthesis by the T4 and T7 holoenzymes was rapid and processive with only a slight dependence on the applied force. An analysis of the primer extension rate as a function of the force estimated a polymerase kinetic step size of ~1 nt for both holoenzymes. On the other hand, the strand displacement activity of the T4 and T7 holoenzymes presented a complex phenomenology (Figure 1C). We found that a large assisting force (>10 pN) was necessary for both the T4 and T7 holoenzymes to replicate the DNA hairpin substrate at their maximum synthesis rates of 200 and 500 nt/s, respectively. Holoenzyme stalling and pausing became the predominant behaviour observed when assisting with moderate forces (~9 pN). At low-assisting forces (<8 pN), the behaviour of the two wt holoenzymes changed to a processive exonuclease activity inhibiting any elongation of the primer. Three different phases, synthesis, degradation and pausing, could easily be identified in the instantaneous velocity distributions (14). The ratio between the three phases was strongly dependent on the applied force (Figure 1D) indicating that the force significantly altered the equilibrium between the holoenzyme–DNA conformations responsible for DNA synthesis, DNA degradation and pausing.

The exo T4 holoenzyme presented very low strand displacement activity of ~1 nt/s at low forces (Supplementary Figure S3A), suggesting that the inefficient strand displacement activity of the wt holoenzymes is not a direct consequence of the exonuclease activity. Our detailed study of the holoenzymes presented elsewhere (14) demonstrates that at low applied forces the DNA fork regression caused polymerization by the holoenzymes to stall. In this situation, the *exo* conformation (i.e. the DNA–polymerase conformation with the primer located at the **exo** active site) was favoured over the *pol* conformation (i.e. the DNA–polymerase conformation with the primer engaged in the **pol** active site) and the newly synthesized DNA strand was degraded at 100 nt/s until the fork reached a region where the ssDNA tails are non-complementary. The polymerase stalling induced by the fork regression pressure and the consequent *pol-exo* equilibrium switch is responsible for the low efficiency of strand displacement DNA synthesis exhibited by these replicative polymerases (14).

Φ29 replicative polymerase as an efficient replisome

The Φ29 polymerase is an active polymerase that performs slow, but processive strand displacement DNA synthesis in the absence of accessory proteins (18). We found that the Φ29 polymerase replicates the DNA predominantly independently of the applied force at a constant rate of ~60 nt/s under our experimental conditions (Supplementary Figure S1). Moreover, in contrast to the T4 or T7 holoenzyme, its DNA synthesis rate was not affected much by the presence of the DNA duplex upstream of the polymerase. Along the range of forces studied, the strand displacement synthesis rate nearly coincided with the primer extension rate, indicating that this polymerase is extremely efficient at performing strand displacement synthesis.

T4 helicase slippage

We have previously demonstrated the ability of the T4 helicase to unwind a DNA hairpin and continue translocating on the ssDNA followed by reannealing of the hairpin behind the helicase (Figure 2A) (17,19). The gp41 helicase translocated rapidly along ssDNA (600 nt/s at 37°C) independently of the applied force (Supplementary Figure S2A). In contrast, the gp41 unwinding activity was strongly force-dependent with the unwinding rate increasing almost exponentially with the applied force. In particular, the helicase unwound the DNA hairpin about six times slower at low force (4–5 pN) than its maximum translocation rate along ssDNA. The helicase also occasionally paused at regions of high GC content during its unwinding activity demonstrating that the DNA sequence affected the helicase activity (Supplementary Figure S2B). This strong force and

sequence dependence revealed that gp41 relies, at least partially, on the thermal fraying of base pairs in order to unwind the DNA fork, which has been associated with the mainly passive character of this helicase (17,19).

We have made the new observation of tens to hundreds of base pairs suddenly reannealing during an unwinding phase (Figure 2B). The unwinding activity immediately before and after these rapid reannealing events observed at low helicase concentration (so that one unwinding event was observed every tens of minutes) supports the conclusion that the same helicase complex remained bound to the DNA. We propose that these rapid reannealing events were generated by the regression pressure of the DNA fork pushing the helicase backwards while attempting to unwind the DNA hairpin. We refer to this phenomenon as helicase slippage. Helicase slippage was initially introduced by Delagoutte and von Hippel (5) as ATP hydrolysis events that resulted from a helicase advancing by less than one full translocation step size (e.g. 1 nt) (20). Here, we extend this concept to include the helicase sliding backwards. The helicase exhibited slippage behaviour most often when unwinding highly stable DNA regions, such as GC-rich regions, at low applied forces and at low ATP concentrations (Figure 2C and D). In particular, the helicase advanced on average less than 100 bp before slipping backwards when the applied force was <5 pN. The dependence on the ATP concentration suggests that slippage events were related to a low-affinity-for-DNA state of the helicase (e.g. a helicase conformation that has partially or completely lost contact with the DNA, but retains the ring-like-shape that prevents dissociation). Helicase slippage has recently been observed for the T7 helicase (21) and such low-affinity-for-DNA states have been proposed for the T7 helicase as part of its ATP-hydrolysis cycle (22). Our results suggest that the fork regression pressure acting on the low-affinity-for-DNA state of the helicase not only reduced its forward motion as previously proposed (5,20), but also induced the helicase to slide backwards. Overall, we conclude that the helicase activity at low force (or in the absence of an external force) is not only limited by its passive character, but also by its tendency to slip backwards.

ssDNA-binding protein gp32 enhances the activities of the holoenzyme and helicase

A replisome is comprised of many proteins working together to replicate the DNA; consequently, some of these other proteins might play a role in modulating the activity of the holoenzyme and helicase. In particular, gp32 is the single-stranded DNA-binding protein in T4 responsible for coating the ssDNA as it is unwound making it essential for lagging-strand synthesis (23); is known to interact directly with several replisome proteins including gp43 polymerase, gp45 clamp, gp59 helicase loader and gp61 primase (24–26).

In the presence of gp32, which shifts the ssDNA $\leftrightarrow$ dsDNA equilibrium towards ssDNA, the regression pressure of the DNA fork junction might be reduced resulting in the stimulation of the strand displacement synthesis by the holoenzyme. Indeed, addition of gp32 to our wt and exo T4 holoenzyme strand displacement synthesis assay shows the almost complete suppression of the processive exonuclease activity and a significant decrease in the holoenzyme stalling behaviour (Supplementary Figure S3A).

On the other hand, the presence of gp32 completely arrested the T4 helicase slippage detected within our spatial resolution ($\sim$10 nt). We attribute this affect to both the ability of gp32 to shift the ssDNA $\leftrightarrow$ dsDNA equilibrium towards ssDNA thereby reducing the regression pressure of the fork junction pushing back on the helicase and to the cooperative binding of gp32 to coat the ssDNA behind the helicase. In addition, the T4 helicase unwinding rate computed from the sections of the experimental traces without detected slippage was increased by a factor of 1.5 at low applied forces (Supplementary Figure S3B). Such a modest stimulation of the unwinding rate suggests that small helicase slippage events (<10 nt), which could not be directly detected, occurred infrequently.

T4 holoenzyme and helicase couple for rapid and processive leading-strand DNA synthesis

In the presence of the wt or exo T4 holoenzyme and T4 helicase, rapid and processive DNA synthesis of the first half of the DNA hairpin was observed at forces <6 pN (Figure 3A). A pause in synthesis occurred when the two enzymes collided head-to-head on the DNA, an artefact created by our hairpin substrate design; eventually the synthesis of the remaining part of the hairpin substrate was completed in the primer extension mode. The rate of this rapid and processive DNA synthesis was $\sim$300 nt/s and independent of the force or presence of gp32; however, it was observed only over the low force range of 1–6 pN (Figure 3C). This fast replication rate was necessarily the result of coupled holoenzyme-helicase activity since the strand displacement and unwinding rates of the isolated enzymes were much slower ($\sim$−100 nt/s or $\sim$1 nt/s for the wt or exo holoenzyme, respectively and $\sim$100 bp/s for the helicase) and strongly force dependent over this force range (Figure 3C). In contrast, the T4 holoenzyme and helicase activities were clearly uncoupled at forces >7 pN; experimental traces exhibited rapid bursts of helicase unwinding activity and separate or trailing DNA synthesis by the holoenzyme in the strand displacement or primer extension mode (Figure 3B). Uncoupled behaviour could also be induced at forces <5 pN by decreasing the concentration of dNTPs to slow down the synthesis rate of the holoenzyme to well below the unwinding rate of the helicase (Supplementary Figure S4). These results demonstrate that while the coupling between the holoenzyme and helicase produced very efficient stimulation of their separate enzyme activities, any direct physical interaction between the holoenzyme and helicase was weak and could be broken under conditions where the helicase moved faster than the holoenzyme.

By changing the concentration of ATP or dNTPs, we could independently control the maximum rate of

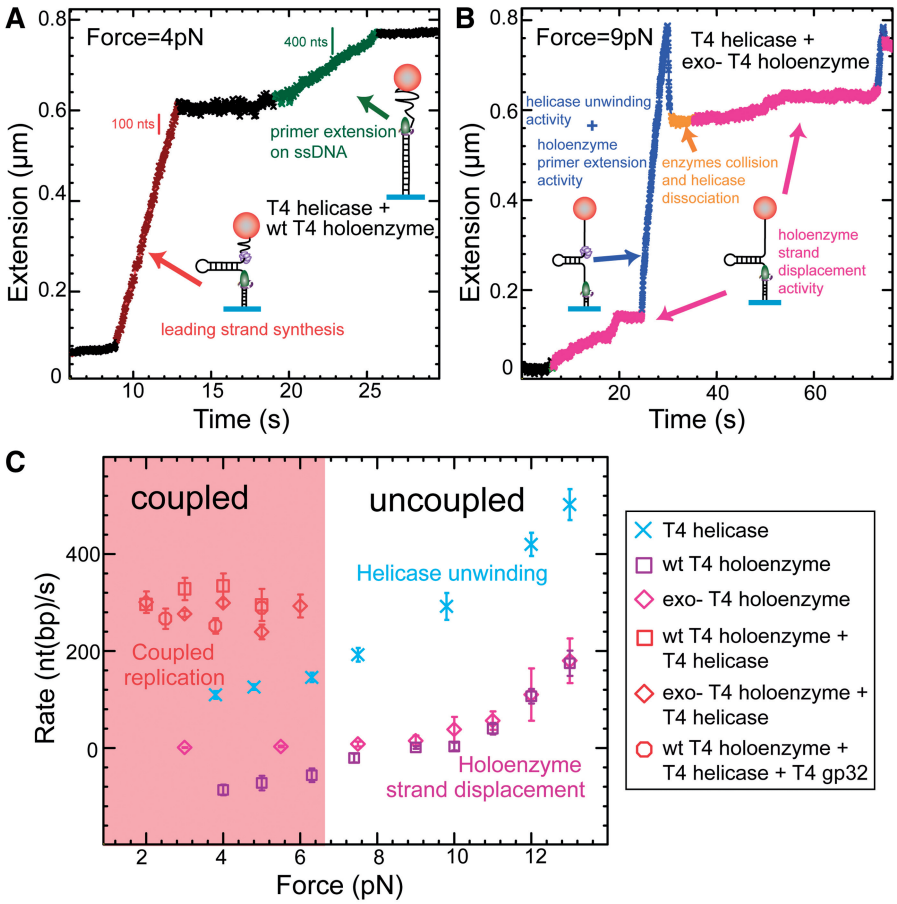

Figure 3. Homologous coupling of the T4 holoenzyme and helicase. (**A**) Experimental trace exhibiting coupled leading-strand DNA synthesis (red) by the wt holoenzyme and helicase at 4 pN followed by a long pause resulting from the collision of the two enzymes at the end of the hairpin and eventual completion of the DNA synthesis by primer extension (green). Bars show the extension change corresponding to the synthesis of 100 and 400 nt for the leading-strand synthesis and the primer extension reactions, respectively. (**B**) Experimental trace exhibiting the uncoupled exo holoenzyme strand displacement activity (magenta) and helicase unwinding activity (blue) at 9 pN of applied force. Initially, the holoenzyme loads and begins DNA synthesis in the strand displacement mode. When the helicase loads, it unwinds the DNA faster than the holoenzyme synthesizes the DNA, passes the loop apex and begins translocating along the leading strand, and collides with the holoenzyme (orange). (**C**) The rate of helicase unwinding, wt and exo holoenzyme strand displacement synthesis and coupled replication in the absence and presence of ssDNA-binding protein are shown as a function of the applied force. Efficient coupling only occurred below 6 pN. Error bars are the SEM. The number of molecules analysed varies depending on the force and conditions between N_{mol} = 25–43, N_{mol} = 9–27 and N_{mol} = 6–21 for the T4 helicase, wt and exo T4 holoenzymes, respectively. For the coupling reaction the number of molecules analysed varies between N_{mol} = 18–30, N_{mol} = 15–22 and N_{mol} = 12–17 for the wt T4 holoenzyme in the absence and presence of gp32 and for the exo T4 holoenzyme, respectively.

either the helicase or holoenzyme, respectively, and investigate the relationship between the coupled replication rate V_{rep}, and the rates of each individual enzyme, V_{hel}^{T} and V_{pol}^{PE}. Supplementary Figure S4 shows how V_{rep}, V_{hel}^{T} and V_{pol}^{PE} varied with the ATP or dNTP concentration demonstrating that both enzymes modulated the replication rate with the maximum rate being limited by the slowest enzyme.

Coupling does not require a homologous system but not all the heterologous systems couple

Previous studies have shown that heterologous combinations of holoenzymes and helicases from T4 and T7 could perform coupled leading-strand DNA synthesis (5,6). Here, we have tested two heterologous polymerases, the T7 holoenzyme and the Φ29 polymerase (Supplementary Figure S5). When testing the pairing of the T7 holoenzyme and the T4 helicase, results similar to the T4 homologous system were obtained: rapid and processive coupled leading-strand DNA synthesis at low forces and uncoupled holoenzyme and helicase activities at high forces. The coupled replication rate of the T7/T4 heterologous system was faster (~400 nt/s) than that measured for the T4 homologous system (~300 nt/s), consistent with the faster primer extension rate for the T7 holoenzyme (14). Nevertheless, the coupled rate of the T7/T4 combination was less than the primer extension rate of the T7 holoenzyme (~500 nt/s). The T7/T4 heterologous system also presented periods of uncoupled behaviour or incomplete replication suggesting that, while heterologous coupling is possible, the homologous proteins work more efficiently together than the heterologous proteins.

In contrast no coupled leading-strand DNA synthesis was observed between the Φ29 polymerase and the T4 helicase (Supplementary Figure S5B). The uncoupling

between Φ29 polymerase and T4 helicase appeared similar to the observations for the T4 homologous system at high forces; in both situations the maximum polymerization rate of the holoenzyme/polymerase was slower than the T4 helicase unwinding rate.

DISCUSSION

This work has attempted to understand the mechanism of functional coupling between replicative holoenzyme complexes responsible for DNA synthesis and helicases responsible for unwinding duplex DNA to produce rapid and processive strand displacement synthesis which mimics leading-strand DNA synthesis in a replisome. By using the T4 bacteriophage as a model system, we first tested the activity of the individual enzymes and found that their unwinding or strand displacement activities were very low when not assisted by force. In stark contrast, the T4 homologous coupled system was very efficient at low forces and DNA synthesis advanced at the maximum rate without exhibiting fork regression or pauses. We modelled the individual enzyme behaviours and propose a collaborative model to best explain the homologous and heterologous coupling results under various experimental conditions.

The helicase is less efficient than the holoenzyme in destabilizing the DNA fork

Betterton and Jülicher (15,16) proposed a framework to describe DNA unwinding by helicases that has been used in several investigations of helicases (17,27,28) and extended to describe strand displacement synthesis of a polymerase, HIV reverse transcriptase (29). In a simplified view, the motor protein moves along ssDNA at a given constant rate V_{ssDNA} (i.e. V_{hel}^{T} ssDNA translocation rate for helicase and V_{pol}^{PE} primer extension rate for holoenzyme). Encountering a DNA fork presents a barrier to the movement of the motor protein possibly changing its rate V_{dsDNA} (i.e. V_{hel}^{UN} unwinding rate for helicase and V_{pol}^{SD} strand displacement synthesis rate for holoenzyme). An active motor protein efficient at reducing the barrier by destabilizing the DNA duplex could move at the same rate on either ssDNA or dsDNA. A passive motor protein inefficient at reducing the barrier must rely on the transient opening fluctuations of the upstream DNA duplex and therefore would move slower on dsDNA than on ssDNA. The force dependence of the ratio between the velocity of the motor protein on dsDNA and ssDNA ($V_{\mathrm{dsDNA}}/V_{\mathrm{ssDNA}}$) is a measure of how efficiently the motor protein resolves the barrier and a way to assess the characteristics of the motor protein.

In this model, the kinetics of the enzyme are governed by the set of parameters including the base pair opening and closing rates, α and β; the enzyme's intrinsic forward and backward translocation rates along ssDNA, k^{+} and k^{-}; the enzyme step size, n; and the enzyme's DNA-destabilization potential, described by the free energy of DNA-enzyme destabilization, ΔG_a and the range of the DNA–enzyme interaction, m (Figure 4A). Active and passive enzymes are characterized, respecitively, by large and small values of ΔG_a as compared to the free energy of formation of a base pair ($\sim 2\ K_B T$ under the experimental conditions). A detailed description of the modelling is given in the Supplementary Materials.

Modelling of the unwinding activity, excluding helicase slippage, best characterized the T4 helicase as a mainly passive ($0.4 \leq \Delta G_a \leq 0.8\ K_B T$ and $1 \leq m \leq 3$ nt), unidirectional motor ($k^{-}/k^{+} < 0.05$) with a step size of 1 nt (Figure 4B and Supplementary Figure S6). The implication is that the T4 helicase must rely on the transient opening of the base pair at a fork in order to step forward due to its inefficiency at destabilizing the upstream DNA duplex.

Modelling of the T4 and T7 holoenzyme polymerization activity, excluding pausing and exonuclease activity, best characterized the holoenzymes as strongly active motors ($1.4 \leq \Delta G_a \leq 1.8\ K_B T$; $3 \leq m \leq 6$ nt and $1.6 \leq \Delta G_a \leq 2\ K_B T$; $2 \leq m \leq 5$ nt for the T4 and T7 holoenzymes, respecitvely) with a step size of 1 nt (Figure 4B and Supplementary Figure S6). This characterization might seem at odds with the processive exonuclease activity exhibited by these holoenzymes in a strand displacement configuration. By excluding holoenzyme pausing and exonuclease activity from our analysis, we effectively modelled the behaviour of the holoenzymes only in the *pol* conformation and excluded the inactive or stalled *I* intermediate and *exo* conformations (14). The implication is that the T4 and T7 holoenzymes are active motor proteins efficient at destabilizing the upstream DNA duplex if the *pol-exo* equilibrium can be shifted towards the *pol* conformation.

Crystal structures of RB69 (a structural and functional T4 homolog) and other polymerases bound to a primed DNA molecule (30,31) give some insight into the possible mechanism for base pair destabilization. The 5′ end of the template strand is bent at almost 90° between the dsDNA primer/template region and the ssDNA template region exiting the polymerase in order to expose the template bases toward the **pol** active site where the 3′ end of the primer is stabilized for extension. This sharp kink in the template strand produces a stress, due to the intrinsic rigidity of the ssDNA, which could propagate along the template strand destabilizing the upstream DNA duplex. Note that the range of the DNA–polymerase interaction estimated from our modelling (m = 3–6 nt) is consistent with results presented in the companion article (14) suggesting that holoenzyme stalling is prevented by the disruption of the first 4–5 bp of the DNA fork.

Helicase–polymerase coupling

The most obvious mechanism to explain the dramatic increase in DNA synthesis and unwinding rates and processivity of the coupled reaction is a direct protein–protein interaction that leads to an allosteric effect stimulating one or both of the enzyme activities. While several groups have searched, no physical interaction between the gp43 polymerase and the gp41 helicase has been detected by analytical ultracentrifugation (5) or by protein–protein cross-linking (32). The T7 holoenzyme and helicase exhibit similar rapid and processive coupled

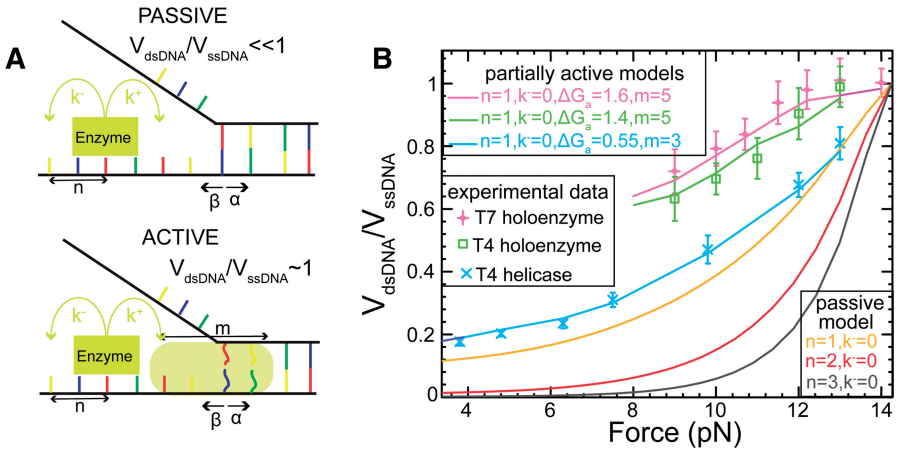

Figure 4. Model for passive and active enzymes. (**A**) Sketch illustrating the parameters used for characterizing a passive (upper) or active (lower) enzyme according to the Betterton and Jülicher model: α and β are the base pair opening and closing rates; k^+ and k^- are the forward and backwards ssDNA translocation rates; n is the enzyme step size and m is the range of the protein–DNA interaction potential. (**B**) Experimentally measured values of V_{dsDNA}/V_{ssDNA} for the T4 helicase (blue crosses), the T4 holoenzyme (green squares) and the T7 holoenzyme (pink pluses) as a function of the applied force are compared to Monte–Carlo simulations of the model for a passive enzyme with various step sizes (yellow, red and grey lines) and an active enzyme (pink, light green and blue lines). Error bars are the SEM. The number of molecules analysed varies depending on the condition between N_{mol} = 25–43, N_{mol} = 9–17 and N_{mol} = 8–15 for the T4 helicase, wt T4 and T7 holoenzymes, respectively.

strand displacement synthesis and share a direct protein–protein interaction through patches of basic residues on the polymerase and the C-terminal tail of the helicase (33,34); however, Stano *et al.* (6) have shown through experiments with T7 helicase truncation mutants lacking the C-terminal tail that the coupled holoenzyme and helicase rate stimulation does not rely on these specific interactions. Moreover, the presence of heterologous coupling between the T4 and T7 enzymes and the force induced uncoupling observed in our assays also argues against a strong specific binding as the mechanism for coupling, but does not rule out a non-specific association of the involved proteins.

Prevention of helicase slippage by the polymerase is not the driving force of the coupling

Delagoutte and von Hippel (5) proposed that a 'trailing' DNA polymerase could prevent strand reannealing and diminish helicase slippage as a mechanism to explain the dramatic increase in unwinding rate and processivity of the coupled reaction, although they had no direct evidence of helicase slippage at the time. The emergence of single-molecule techniques to monitor the activity of individual enzymes has permitted us to obtain direct evidence of the T4 helicase slipping backwards tens to hundreds of base pairs due to the regression pressure of the DNA hairpin substrate. The ssDNA-binding protein gp32, which coats ssDNA, should be able to serve the same function as a 'trailing' polymerase to prevent strand reannealing and slippage by the T4 helicase. Despite the fact that, *a priori*, the holoenzyme might be more efficient than gp32 at preventing strand reannealing since the holoenzyme moves forward in single nucleotide steps and gp32 requires an 8-nt gap for binding, the addition of gp32 to our helicase unwinding assays completely inhibited helicase slippage within our spatial resolution (~10 nt). Additionally, our analysis of the force-dependent helicase unwinding rate is only consistent with a strongly unidirectional motor ($k^-/k^+ \leq 0.05$) implying that small slippage events (<10 nt) are rare and contribute little to the overall unwinding rate. Therefore, the modest stimulation of the unwinding rate, still well below the ssDNA translocation rate of the T4 helicase or the coupled strand displacement rate, indicates that preventing helicase slippage alone cannot account for the processivity and rate enhancement of the coupled holoenzyme and helicase.

Stano *et al.* (6) proposed that DNA synthesis and rapid trapping of the ssDNA bases by the polymerase provided the driving force to accelerate duplex unwinding resulting in rapid and processive leading-strand synthesis in the T7 system. In agreement with this scenario, we found that the synthesis rate of the coupling reaction is controlled by the holoenzyme polymerization rate. However, our results also point out the importance of the helicase at the replication fork, not only to provide ssDNA template for the holoenzyme, but also to relieve the fork regression pressure on the holoenzyme preventing holoenzyme stalling. The almost complete suppression of the processive exonuclease activity and decrease in the holoenzyme stalling behaviour by the addition of gp32, which shifts the ssDNA ↔ dsDNA equilibrium towards ssDNA thereby reducing the fork regression pressure, to our strand displacement synthesis assay illustrates this point.

A collaborative model mediated through the DNA accurately reproduces the experimental results

The collaborative coupling model proposed here is based on the idea that the two individual enzymes assist each other to maximize the efficiency of their combined activity. To characterize coupled leading-strand DNA

synthesis, we combined the separate models used to describe helicase unwinding and holoenzyme polymerization. Details of the model are presented in the Supplementary Materials and Supplementary Figure S6. Because of the random assembly of the enzymes on the DNA fork, the relative position of the two enzymes was not imposed *a priori* and both possibilities were evaluated. However, we presumed that the presence of the DNA fork affected only the enzyme in the leading position. In other words, the DNA fork only represented an extra energetic barrier for the advance of the leading enzyme, while the trailing enzyme could advance freely on ssDNA. If the helicase were ahead of the holoenzyme, then the helicase was allowed to move forward and backwards in response to the fork pressure, but the holoenzyme was considered to remain in the active *pol* state. In the opposite situation, when the holoenzyme was in the leading position transitions from the *pol* state to the *exo* state of the holoenzyme were allowed.

Modelling of the coupled leading-strand DNA synthesis best characterized the relationship between the T4 or T7 holoenzyme and the T4 helicase as a collaboration between an active ($\Delta G_a \sim 1.6\ K_BT$; $m \sim 4$ nt and $\Delta G_a \sim 1.8\ K_BT$; $m \sim 4$ nt for the T4 and T7 holoenzymes, respectively) holoenzyme and a mainly passive ($\Delta G_a \sim 0.6\ K_BT$ and $m \sim 3$ nt) T4 helicase, both localized at the replication fork with the helicase slightly closer to the fork junction (Figure 5A). By unwinding the DNA duplex and providing ssDNA template, the helicase apparently prevents the holoenzyme from stalling thereby stimulating the DNA synthesis. Kept persistently in the *pol* conformation by the presence of the helicase at the replication fork, the holoenzyme stimulates the helicase unwinding rate and prevents helicase slippage. We, however, with the present data cannot comment on the exact number DNA base pairs destabilized or how it is achieved. The stimulation of both enzyme activities is mediated through the DNA and no specific strong protein–protein interaction is necessary allowing for homologous and heterologous coupling of holoenzymes and helicases to produce rapid and processive strand displacement activity so long as the polymerase primer extension rate is faster than the helicase unwinding rate.

Our collaborative model for coupled leading-strand DNA synthesis can be used to accurately reproduce our experimentally obtained results. For example, our model predicts that below ~8 pN of applied force the coupled replication rate should be force independent and that above ~8 pN of applied force the two enzymes should become uncoupled due to the fact that the helicase unwinding rate exceeds the maximum primer extension rate at these forces, which agrees with what we observed (Figure 5B). In the absence of a structure of the assembled DNA–protein complex, we cannot comment on the significance of the uncoupling occurring at ~8 pN. Although not explicitly shown in Figure 5A the polymerase is associated with the gp45 clamp protein that may dissociate in response to an applied force. According to our collaborative model, the coupled replication rate should be limited by the rate of the slowest enzyme under the experimental conditions. By varying the ATP and dNTP concentrations, we were able to show that the coupled replication rate was indeed limited by the rate of helicase unwinding at low ATP concentrations and by the rate of DNA synthesis at low dNTP concentrations (Figure 5C and Supplemental Figure S4). Lastly, the collaborative model accurately simulated a faster coupled replication rate for the T7/T4 heterologous pair than the T4/T4 homologous pair (Figure 5C), consistent with the faster primer extension rate of the T7 holoenzyme than the T4 holoenzyme, and the lack of coupling between the Φ29 polymerase and T4 helicase.

Generality of the collaborative strategy in replication systems

The two main elements of the collaborative model are the prevention of the holoenzyme stalling by the presence of the helicase at the DNA fork and the holoenzyme induced destabilization of the DNA fork that stimulates helicase unwinding. These two elements are most probably present in many replicative systems; on the one hand, replicative helicases are hexameric ring-like enzymes that encircle one strand of the DNA while stericly excluding the complementary strand; on the other hand, results obtained with different replicative holoenzymes show that, when stabilized in the *pol* active conformation, the polymerase is able to efficiently destabilize the DNA duplex. Therefore, the collaborative model proposed here likely describes a general strategy in leading-strand coupling. This collaborative strategy may give the replisome the needed flexibility to coordinate leading- and lagging-strand synthesis and, at the same time, provide the tight coupling that prevents replisome disassembly.

The collaborative model between helicases and holoenzymes that we propose is not exclusive and does not preclude additional specific protein interactions or protein interaction networks to promote rapid DNA replication by replisomes. In other well-studied replication systems, such as the *E. coli* system, protein interactions have been shown to play important roles in enhancing the rate of replication. For instance, the direct interaction of the χ subunit of the Pol III holoenzyme with SSB bound on the lagging DNA strand stabilizes the leading-strand polymerase resulting in strand displacement synthesis (35). Also, a specific interaction between the τ subunit of the Pol III holoenzyme and the DnaB helicase stimulates the unwinding rate of the helicase over 10-fold (36).

The present quantitative analysis can be applied to other replicative systems in order to test the generality of the strategy proposed. Mutations on the helicase and polymerase proteins that may potentially affect their DNA destabilizing ability, and accordingly their coupling, would provide an interesting test for further validating the model.

SUPPLEMENTARY DATA

Supplementary Data are available at NAR Online: Supplementary Figures 1–6, Supplementary Materials and Supplementary References [37–39].

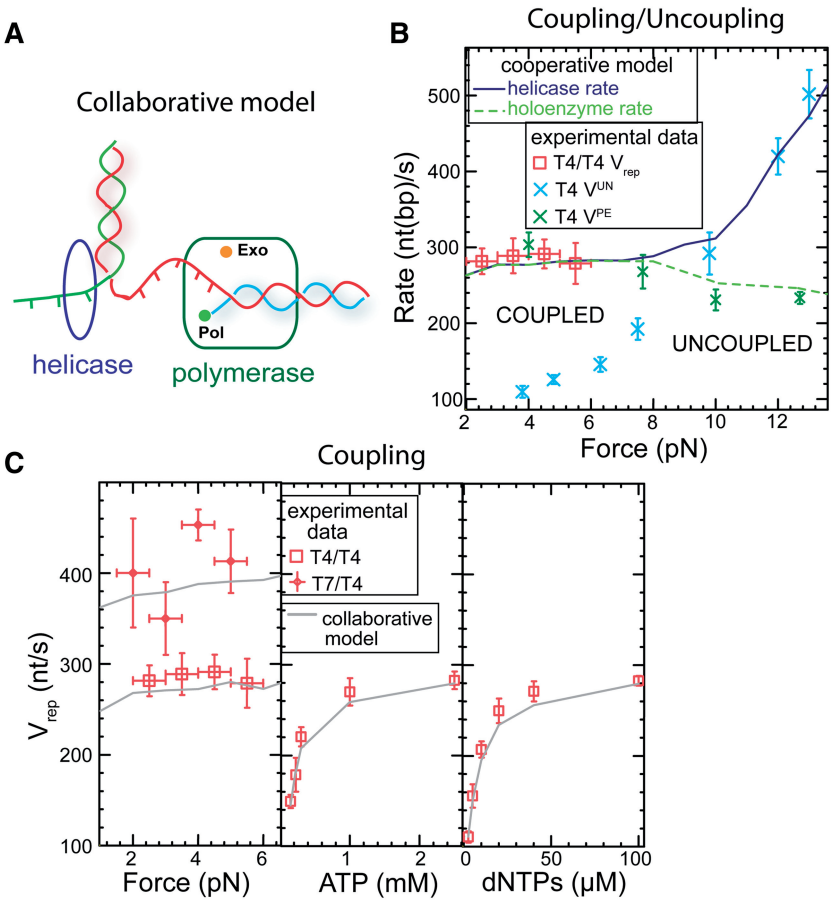

Figure 5. Collaborative model for leading-strand DNA synthesis. (**A**) Diagram representing the coupling of the T4 holoenzyme and helicase in which the holoenzyme destabilizes the first few base pairs of the duplex DNA to enhance the helicase unwinding and the helicase prevents the base pair from reannealing thereby maintaining the holoenzyme in the polymerization conformation. (**B**) Helicase unwinding rate (blue line) and holoenzyme strand displacement synthesis rate (green dashed line) obtained from Monte–Carlo simulations based on the collaborative coupling model with a mainly passive helicase ($\Delta G_a = 0.55\ K_BT$ and $m = 3$ nt) and strongly active holoenzyme ($\Delta G_a = 1.6\ K_BT$ and $m = 4$ nt). Results present a region of coupling at low forces where $V_{hel}^{UN} = V_{pol}^{SD}$, that compare well with the measured rates for homologous T4 coupled replication V_{rep} (red symbols), and a region of uncoupling at high forces where $V_{hel}^{UN} > V_{pol}^{SD} \sim V_{pol}^{PE}$. The measured T4 helicase unwinding V_{hel}^{UN} (light blue symbols) and T4 holoenzyme primer extension V_{pol}^{PE} (green symbols) are shown for comparison. Error bars are the SEM. The number of molecules analysed varies depending on the conditions between $N_{mol} = 25$–43, $N_{mol} = 10$–23 and $N_{mol} = 18$–30 for the T4 helicase, wt T4 holoenzyme and T4/T4 coupled replication system, respectively. (**C**) Comparisons between simulated (grey lines) and experimental (red symbols) results for the coupled replication rates V_{rep} as a function of force (left panel); ATP concentration (central panel) and dNTP concentration (right panel) are shown. Parameters used in the model are ($\Delta G_a = 0.55\ K_BT$ and $m = 3$ nt for the helicase, $\Delta G_a = 1.6\ K_BT$ and $m = 4$ nt, and $\Delta G_a = 1.9\ K_BT$ and $m = 3$ nt for the T4 and T7 holoenzymes, respectively. Error bars are the SEM. The number of molecules analysed varies between $N_{mol} = 18$–30 (left panel), $N_{mol} = 7$–26 (central panel) and $N_{mol} = 9$–26 (right panel) for the T4/T4 coupled replication system and between $N_{mol} = 14$–23 for the T7/T4 coupled replication system.

ACKNOWLEDGEMENTS

We would like to thank B. Ibarra for discussions on the work and reading of the manuscript and M. Baaden for stimulating discussions.

FUNDING

Human Frontier Science Program [RGP0003/2007-C] to V.C. and S.J.B.; National Institutes of Health [GM013306] to S.J.B.; European Research Council [MAGREPS 267 862] to V.C. Funding for open access charge: European Research Council [MAGREPS 267 862].

Conflict of interest statement. None declared.

REFERENCES

1. Benkovic,S.J., Valentine,A.M. and Salinas,F. (2001) Replisome-mediated DNA replication. *Annu. Rev. Biochem.*, **70**, 181–208.
2. Venkatesan,M., Silver,L.L. and Nossal,N.G. (1982) Bacteriophage T4 gene 41 protein, required for the synthesis of RNA primers, is also a DNA helicase. *J. Biol. Chem.*, **257**, 12426–12434.
3. Hacker,K.J. and Alberts,B.M. (1994) The rapid dissociation of the T4 DNA polymerase holoenzyme when stopped by a DNA hairpin helix. A model for polymerase release following the termination of each Okazaki fragment. *J. Biol. Chem.*, **269**, 24221–24228.
4. Cha,T.A. and Alberts,B.M. (1989) The bacteriophage T4 DNA replication fork. Only DNA helicase is required for leading strand DNA synthesis by the DNA polymerase holoenzyme. *J. Biol. Chem.*, **264**, 12220–12225.
5. Delagoutte,E. and von Hippel,P.H. (2001) Molecular mechanisms of the functional coupling of the helicase (gp41) and polymerase

(gp43) of bacteriophage T4 within the DNA replication fork. *Biochemistry*, **40**, 4459–4477.
6. Stano,N.M., Jeong,Y.J., Donmez,I., Tummalapalli,P., Levin,M.K. and Patel,S.S. (2005) DNA synthesis provides the driving force to accelerate DNA unwinding by a helicase. *Nature*, **435**, 370–373.
7. Frey,M.W., Nossal,N.G., Capson,T.L. and Benkovic,S.J. (1993) Construction and characterization of a bacteriophage T4 DNA polymerase deficient in 3′–>5′ exonuclease activity. *Proc. Natl Acad. Sci. USA*, **90**, 2579–2583.
8. Nossal,N.G. (1979) DNA replication with bacteriophage T4 proteins. Purification of the proteins encoded by T4 genes 41, 45, 44, and 62 using a complementation assay. *J. Biol. Chem.*, **254**, 6026–6031.
9. Rush,J., Lin,T.C., Quinones,M., Spicer,E.K., Douglas,I., Williams,K.R. and Konigsberg,W.H. (1989) The 44P subunit of the T4 DNA polymerase accessory protein complex catalyzes ATP hydrolysis. *J. Biol. Chem.*, **264**, 10943–10953.
10. Valentine,A.M., Ishmael,F.T., Shier,V.K. and Benkovic,S.J. (2001) A zinc ribbon protein in DNA replication: primer synthesis and macromolecular interactions by the bacteriophage T4 primase. *Biochemistry*, **40**, 15074–15085.
11. Nelson,S.W., Kumar,R. and Benkovic,S.J. (2008) RNA primer handoff in bacteriophage T4 DNA replication: the role of single-stranded DNA-binding protein and polymerase accessory proteins. *J. Biol. Chem.*, **283**, 22838–22846.
12. Manosas,M., Spiering,M.M., Zhuang,Z., Benkovic,S.J. and Croquette,V. (2009) Coupling DNA unwinding activity with primer synthesis in the bacteriophage T4 primosome. *Nat. Chem. Biol.*, **5**, 904–912.
13. Gosse,C. and Croquette,V. (2002) Magnetic tweezers: micromanipulation and force measurement at the molecular level. *Biophys. J.*, **82**, 3314–3329.
14. Manosas,M., Spiering,M.M., Ding,F., Bensimon,D., Allemand,J.-F., Benkovic,S.J. and Croquette,V. (2012) Mechanism of strand displacement synthesis by DNA replicative polymerases. *Nucleic Acids Res.*, **40**, 6174–6186.
15. Betterton,M.D. and Julicher,F. (2003) A motor that makes its own track: helicase unwinding of DNA. *Phys. Rev. Lett.*, **91**, 258103.
16. Betterton,M.D. and Julicher,F. (2005) Opening of nucleic-acid double strands by helicases: active versus passive opening. *Phys. Rev. E Stat. Nonlin. Soft Matter Phys.*, **71**, 011904.
17. Lionnet,T., Spiering,M.M., Benkovic,S.J., Bensimon,D. and Croquette,V. (2007) Real-time observation of bacteriophage T4 gp41 helicase reveals an unwinding mechanism. *Proc. Natl Acad. Sci. USA*, **104**, 19790–19795.
18. Blanco,L., Bernad,A., Lázaro,J.M., Martín,G., Garmendia,C. and Salas,M. (1989) Highly efficient DNA synthesis by the phage phi 29 DNA polymerase. Symmetrical mode of DNA replication. *J. Biol. Chem.*, **264**, 8935–8940.
19. Manosas,M., Xi,X.G., Bensimon,D. and Croquette,V. (2010) Active and passive mechanisms of helicases. *Nucleic Acids Res.*, **38**, 5518–5526.
20. von Hippel,P.H. and Delagoutte,E. (2001) A general model for nucleic acid helicases and their 'coupling' within macromolecular machines. *Cell*, **104**, 177–190.
21. Sun,B., Johnson,D.S., Patel,G., Smith,B.Y., Pandey,M., Patel,S.S. and Wang,M.D. (2011) ATP-induced helicase slippage reveals highly coordinated subunits. *Nature*, **478**, 132–135.
22. Liao,J.C., Jeong,Y.J., Kim,D.E., Patel,S.S. and Oster,G. (2005) Mechanochemistry of T7 DNA helicase. *J. Mol. Biol.*, **350**, 452–475.
23. Chase,J.W. and Williams,K.R. (1986) Single-stranded DNA binding proteins required for DNA replication. *Annu. Rev. Biochem.*, **55**, 103–136.
24. Formosa,T., Burke,R.L. and Alberts,B.M. (1983) Affinity purification of bacteriophage T4 proteins essential for DNA replication and genetic recombination. *Proc. Natl Acad. Sci. USA*, **80**, 2442–2446.
25. Burke,R.L., Munn,M., Barry,J. and Alberts,B.M. (1985) Purification and properties of the bacteriophage T4 gene 61 RNA priming protein. *J. Biol. Chem.*, **260**, 1711–1722.
26. Morrical,S.W., Beernink,H.T., Dash,A. and Hempstead,K. (1996) The gene 59 protein of bacteriophage T4. Characterization of protein-protein interactions with gene 32 protein, the T4 single-stranded DNA binding protein. *J. Biol. Chem.*, **271**, 20198–20207.
27. Johnson,D.S., Bai,L., Smith,B.Y., Patel,S.S. and Wang,M.D. (2007) Single-molecule studies reveal dynamics of DNA unwinding by the ring-shaped T7 helicase. *Cell*, **129**, 1299–1309.
28. Ribeck,N., Kaplan,D.L., Bruck,I. and Saleh,O.A. (2010) DnaB helicase activity is modulated by DNA geometry and force. *Biophys. J.*, **99**, 2170–2179.
29. Kim,S., Schroeder,C.M. and Xie,X.S. (2010) Single-molecule study of DNA polymerization activity of HIV-1 reverse transcriptase on DNA templates. *J. Mol. Biol.*, **395**, 995–1006.
30. Doublié,S., Tabor,S., Long,A.M., Richardson,C.C. and Ellenberger,T. (1998) Crystal structure of a bacteriophage T7 DNA replication complex at 2.2 A resolution. *Nature*, **391**, 251–258.
31. Hogg,M., Wallace,S.S. and Doublie,S. (2004) Crystallographic snapshots of a replicative DNA polymerase encountering an abasic site. *EMBO J.*, **23**, 1483–1493.
32. Ishmael,F.T., Trakselis,M.A. and Benkovic,S.J. (2003) Protein-protein interactions in the bacteriophage T4 replisome. The leading strand holoenzyme is physically linked to the lagging strand holoenzyme and the primosome. *J. Biol. Chem.*, **278**, 3145–3152.
33. Notarnicola,S.M., Mulcahy,H.L., Lee,J. and Richardson,C.C. (1997) The acidic carboxyl terminus of the bacteriophage T7 gene 4 helicase/primase interacts with T7 DNA polymerase. *J. Biol. Chem.*, **272**, 18425–18433.
34. Ghosh,S., Hamdan,S.M., Cook,T.E. and Richardson,C.C. (2008) Interactions of *Escherichia coli* thioredoxin, the processivity factor, with bacteriophage T7 DNA polymerase and helicase. *J. Biol. Chem.*, **283**, 32077–32084.
35. Yuan,Q. and McHenry,C.S. (2009) Strand displacement by DNA polymerase III occurs through a τ-ψ-χ link to single-stranded DNA-binding protein coating the lagging strand template. *J. Biol. Chem.*, **284**, 31672–31679.
36. Kim,S., Dallmann,H.G., McHenry,C.S. and Marians,K.J. (1996) Coupling of a replicative polymerase and helicase: a tau-DnaB interaction mediates rapid replication fork movement. *Cell*, **84**, 643–650.
37. Cocco,S., Marko,J.F. and Monasson,R. (2003) Slow nucleic acid unzipping kinetics from sequence-defined barriers. *Eur. Phys. J. E Soft Matter*, **10**, 153–161.
38. Markham,N.R. and Zuker,M. (2005) DINAMelt web server for nucleic acid melting prediction. *Nucleic Acids Res.*, **33**, W577–W581.
39. Guéron,M. and Leroy,J.L. (1995) Studies of base pair kinetics by NMR measurement of proton exchange. *Methods Enzymol.*, **261**, 383–413.